Photoluminescence of Bridged Silsesquioxanes Containing Urea or Urethane Groups with Nanostructures Generated by the Competition between the Rates of Self-Assembly of Organic Domains and the Inorganic Polycondensation

Diana P. Fasce,[†] Roberto J. J. Williams,*[,†] Libor Matějka,[‡] Josef Pleštil,[‡] Jiří Brus,[‡] Berna Serrano,[§] Juan C. Cabanelas,[§] and Juan Baselga[§]

Institute of Materials Science and Technology (INTEMA), University of Mar del Plata and National Research Council (CONICET), J.B. Justo 4302, 7600 Mar del Plata, Argentina; Institute of Macromolecular Chemistry, Academy of Sciences of the Czech Republic, Heyrovský Sq. 2, 162 06 Prague 6, Czech Republic; and Department of Materials Science and Engineering and Chemical Engineering, Universidad Carlos III de Madrid, 28911 Leganés, Spain

Received September 28, 2005; Revised Manuscript Received March 27, 2006

ABSTRACT: The aim of this study was to investigate the changes produced in the nanostructures and the photoluminescence spectra of bridged silsesquioxanes containing urea or urethane groups, by varying the relative rates between the self-assembly of organic domains and the inorganic polycondensation. Precursors of the bridged silsesquioxanes were 4,4′-[1,3-phenylenebis(1-methylethylidene)]bis(aniline) and 4,4′-isopropylidenediphenol, end-capped with 3-isocyanatopropyltriethoxysilane. The inorganic polycondensation was produced using either high or low formic acid concentrations, leading to transparent films with different nanostructures as revealed by FTIR, SAXS, and ^{29}Si NMR spectra. For the bridged silsesquioxanes containing urea groups the self-assembly of organic domains was much faster than the inorganic polycondensation for both formic acid concentrations. However, the arrangement was more regular and the short-range order higher when the rate of inorganic polycondensation was lower. The photoluminescence spectra of the most ordered structures revealed the presence of two main processes: radiative recombinations in inorganic clusters and photoinduced proton-transfer generating NH_2^+ and N^- defects and their subsequent radiative recombination. In the less-ordered urea-bridged silsesquioxanes a third process was present assigned to a photoinduced proton transfer in H-bonds exhibiting a broad range of strengths. For urethane-bridged silsesquioxanes the driving force for the self-assembly of organic bridges was lower than for urea-bridged silsesquioxanes. When the synthesis was performed with a high formic acid concentration, self-assembled structures were not produced. Instead, large inorganic domains composed of small inorganic clusters were generated. Self-assembly of organic domains took place only when employing low polycondensation rates. For both materials the photoluminescence was mainly due to radiative processes within inorganic clusters and varied significantly with their state of aggregation.

Introduction

Bridged silsesquioxanes are a family of organic−inorganic hybrid materials prepared by the hydrolysis and condensation of monomers containing an organic bridging group joining two (or eventually more) trialkoxysilyl or trichlorosilyl groups.[1−11] The organic group, covalently bonded to the trialkoxysilyl groups, can be varied in composition, length, rigidity, and functionalization. This determines its contribution to the properties of the cross-linked material.

Bridged silsesquioxanes bearing urea or urethane groups have received considerable attention in recent years due to their capacity of self-structuration through H-bonds. The self-assembly capacity of urea groups was used to synthesize hybrid materials with shape-controlled structures such as hollow tubes, spheres, layered sheets, and helical morphologies.[12−17] Long-range ordered hybrids were obtained when hydrogen-bonding interactions were combined with aromatic $\pi-\pi$ or hydrophobic interactions.[17−21]

Another interesting property associated with the presence of urea or urethane groups in these hybrid materials is their white-light photoluminescence.[22−26] Two mechanisms have been identified as responsible for the photoluminescence.[25] A blue-band emission with a maximum at about 480 nm for excitation wavelengths (λ_{exc}) between 320 and 420 nm was ascribed to a photoinduced proton transfer generating NH_2^+ and N^- defects and their subsequent radiative recombination. A red shift of this band was observed for λ_{exc} higher than 430 nm. The quantum yield of this band was quantitatively associated with the extent and magnitude of the supramolecular interactions resulting from the self-assembly of urea or urethane groups via hydrogen bonding. The second mechanism was associated with the presence of a purplish-blue band around 406 nm for $\lambda_{exc} < 330$ nm, with a red shift for λ_{exc} in the range 350−400 nm. This band was assigned to radiative recombinations that occur within the nanometer-sized siliceous clusters associated with oxygen-related defects.[25]

Most of the photoluminescent bridged silsesquioxanes functionalized with urea or urethane groups that are reported in the literature were synthesized employing different diamines or diols reacted with 3-isocyanatopropyltriethoxysilane (IPTS). These precursors were hydrolyzed and condensed under identical experimental conditions, and characteristics of the resulting photoluminescence spectra were correlated with the chemical structure and length of the organic bridge.[25]

* To whom correspondence should be addressed. E-mail: williams@fi.mdp.edu.ar.
[†] INTEMA.
[‡] Institute of Macromolecular Chemistry.
[§] Universidad Carlos III de Madrid.

10.1021/ma052105y CCC: $33.50
Published on Web 04/27/2006

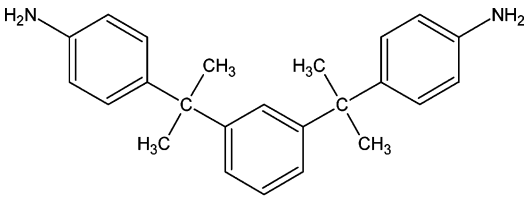

BSA

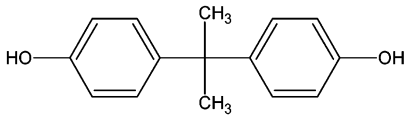

BPA

Figure 1. Chemical structures of BSA and BPA.

In this paper we address a different question related to the way in which the competition between the self-assembly of organic groups and the inorganic polycondensation alters the nanostructuration of a bridged silsesquioxane and the implications that this has on the photoluminescence spectra. Two different families of bridged silsesquioxanes were synthesized. The reaction between an aromatic amine and IPTS led to a precursor with urea groups characterized by a fast self-assembly of organic bridges. The reaction between a bisphenol and IPTS led to a precursor with urethane bridges characterized by a slower self-assembly process. For both precursors the rate of the inorganic polycondensation was varied with the relative amount of formic acid used in the synthesis. In this way a relative control on the ratio of rates of self-assembly of organic bridges and inorganic polycondensation could be achieved. The structures generated were analyzed by Fourier transformed infrared spectra (FTIR), ^{29}Si NMR, and small-angle X-ray scattering (SAXS). Characteristics of the photoluminescence spectra were correlated with the nanostructuration produced in the synthesis.

Experimental Section

Materials. Precursors of the bridged silsesquioxanes were 4,4′-[1,3-phenylenebis(1-methylethylidene)]bis(aniline) (BSA, Ken Seika Corp., 99% purity) and 4,4′-isopropylidenediphenol (Bisphenol A, BPA, Aldrich, 99% purity). The isocyanate was 3-isocyanatopropyltriethoxysilane (IPTS, Fluka, purity >95%). Chemical structures of BSA and BPA are shown in Figure 1.

Reactions were carried out in tetrahydrofuran (THF) that was distilled and recovered over $MgSO_4$ before use. Dibutyltin dilaurate (DBTDL) was used as a catalyst for the synthesis of the urethane. Formic acid (98−100%, Merck) and distilled water were used for the hydrolysis and condensation of the reaction products of ITPS with BSA or BPA.

Synthesis of Bridged Silsesquioxanes. A 0.2 M solution of stoichiometric amounts of IPTS and BSA (or BPA) in THF was held at 50 °C for 48 h. In the case of BPA, DBTDL was added as a catalyst (1.6 g of DBTDL/100 g of BPA) to get a complete conversion of isocyanate groups in a reasonable time. (The reactivity of BPA with an isocyanate is lower than the one of an aliphatic alcohol.) After 48 h the reaction was complete as indicated by the absence of the NCO band at 2273 cm^{-1} in infrared spectra. The reaction between IPTS and BSA led to the urea precursor, and the one between IPTS and BPA originated the urethane precursor (Figure 2).

The hydrolysis and condensation of urea and urethane precursors were performed at room temperature employing 0.1 M solutions in THF (Figure 2). Two different formic acid and water ratios were used as indicated in Table 1. A molar ratio HCOOH/Si = 3

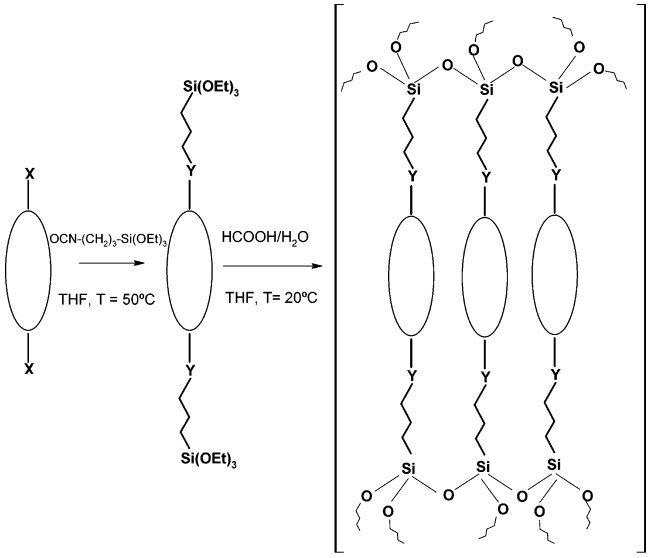

X = -NH$_2$, -OH

Y = -NH-CO-NH-, -NH-CO-O-

Figure 2. Scheme of the synthesis of the bridged silsesquioxanes.

Table 1. Molar Ratios of HCOOH/Si and H_2O/Si Employed for the Synthesis of Bridged Silsesquioxanes (U = Urea; Ut = Urethane)

sample	HCOOH/Si	H_2O/Si
U-1	3	1.5
U-2	0.1	3
Ut-1	3	1.5
Ut-2	0.1	3

produced fast rates of hydrolysis and condensation.[27,28] For these formulations, the stoichiometric amount of water was used, H_2O/Si = 1.5. For formulations synthesized with HCOOH/Si = 0.1 hydrolysis and condensation took place at lower rates. For these samples the amount of added water was the one necessary to produce complete hydrolysis, H_2O/Si = 3.

Solutions were cast in polyacetal recipients of 5 cm diameter with an initial height of liquid close to 5 mm and a glass cover that enabled the control of the solvent evaporation rate. Hydrolysis and condensation reactions took place at room temperature together with solvent evaporation. After about 2 weeks THF was completely evaporated, and the resulting films could be easily detached from the plastic recipient. Films were transparent (the urea products exhibited a slight yellow color), indicating that any structuration was confined to the nanometer range.

FTIR Spectra. Fourier transformed infrared spectroscopy (FTIR, Genesis II, Mattson) was used to characterize precursors (by transmission from solutions cast on NaCl windows) and bridged silsesquioxanes (by attenuated total reflectance of the films).

^{29}Si NMR Spectra. Single-pulse MAS NMR spectra were obtained using a Bruker DSX 200 NMR spectrometer at the frequency of 39.75 MHz. Magic angle spinning (MAS) frequency was 10 kHz and strength of B_1 field (^{1}H, ^{13}C, and ^{29}Si) of 62.5 kHz. The number of scans was 1200−3600. Single-pulse experiments were used with 45° pulse length (2 μs) and 60 s repetition delays. The ^{29}Si scale was calibrated by external standard M_8Q_8 (−109.8 ppm; the highest field signal).

Small-Angle X-ray Scattering (SAXS). SAXS measurements were performed on a Kratky camera with a 60 μm entrance slit and a 42 cm sample-to-detector distance. Ni-filtered Cu Kα radiation (λ = 0.154 nm) was recorded with a linear position-sensitive detector (Joint Institute for Nuclear Research, Dubna, Russia). The experimental (smeared) SAXS curves are presented as a function of the magnitude of the scattering vector $q = (4\pi/\lambda) \sin \theta$ (2θ is the scattering angle).

Photoluminescence Spectra. Measurements were performed on an Edinburgh FS900 spectrofluorimeter with a Xe arc lamp (150 W) with double excitation and emission monochromators. The films

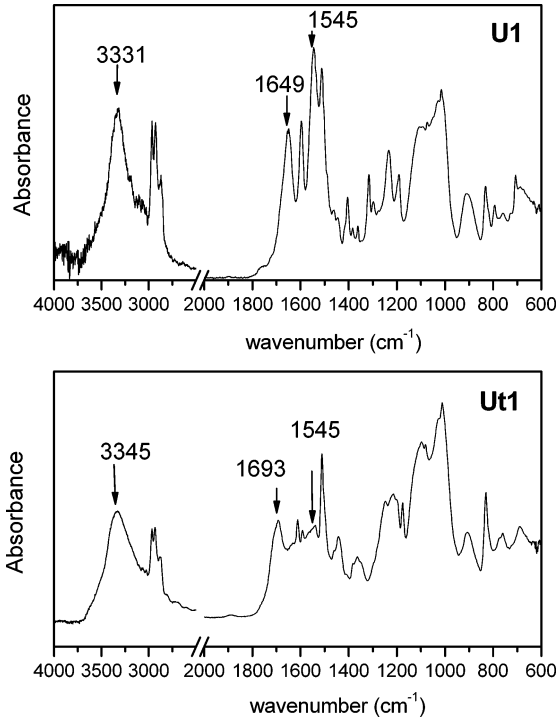

Figure 3. FTIR spectra of U-1 and Ut-1.

Table 2. Characteristic FTIR Bands of Urea- and Urethane-Bridged Silsesquioxanes

sample	N−H stretching (cm^{-1})	amide I region (cm^{-1})	amide II region (cm^{-1})
U-1	3331	1649	1545
U-2	3331	1645	1545
Ut-1	3345	1693	1545
Ut-2	3330	1706	1544

were placed in the sample holder forming an angle of 45° relative to the incident light. Corrected emission spectra were scanned from 330 to 650 nm using excitation wavelengths comprised between 330 and 450 nm. Excitation spectra were recorded for different emission wavelengths. The excitation and emission slits were equal to 1.8 nm. Both emission and excitation spectra were recorded at room temperature with a resolution of 0.5 nm.

Results and Discussion

FTIR Spectra. Figure 3 shows the FTIR spectra of U-1 and Ut-1 synthesized using a high formic acid concentration (high rate of inorganic polycondensation). In both cases, the main changes observed with respect to the FTIR spectra of the precursors were (a) disappearance of characteristic bands of $SiOCH_2CH_3$ groups at 956 and 1166 cm^{-1} (the doublet at 1080 and 1103 cm^{-1} was overlapped with the broad band of Si−O−Si asymmetric stretching vibrations),[29−31] indicating that the hydrolysis of precursors was complete, and (b) appearance of a band at 908 cm^{-1} assigned to SiOH groups,[31] meaning that condensation reactions of silanol groups were not carried out to full conversion. Similar findings were observed for U-2 and Ut-2, synthesized using a low formic acid concentration. The most relevant bands for characterization purposes are indicated in Table 2 for the four samples.

Both urea-bridged silsesquioxanes exhibited characteristic FTIR bands at practically the same frequencies. The broad N−H stretching vibration band at 3331 cm^{-1} is characteristic of hydrogen-bonded N−H groups of varying strength, with a partial contribution of H-bonded SiOH groups.[20,32] Free N−H groups that absorb at about 3445 cm^{-1} [20,33] were not present in significant concentrations.

The C═O stretching vibration in the amide I region is sensitive to the magnitude of hydrogen bonding. In bridged silsesquioxane with flexible organic parts containing urea groups, the band in the amide I region exhibited a maximum at 1643 cm^{-1} for the shorter organic bridge that was upshifted to 1751 cm^{-1} for the longer organic bridge.[32] The band at 1643 cm^{-1} indicates the formation of hydrogen-bonded carbonyl groups while the band at 1751 cm^{-1} corresponds to free carbonyl groups. For amorphous urea-bridged silsesquioxane with 9−12 methylene groups between both urea groups, a broad band of H-bonded C═O groups with a maximum at 1645 cm^{-1} was observed.[20] The broadness of this band was assigned to a nonhomogeneous distribution of hydrogen bonding.[20,26] To analyze the distribution of hydrogen bonding of C═O groups in U-1 and U-2, a spectral deconvolution of this band was performed using the Origin package and Lorentzian band shapes. For U-2 the experimental band could be fitted by a single Lorentzian band with a maximum at 1647 cm^{-1}. For U-1 the experimental band was composed of three Lorentzian bands at 1651 cm^{-1} (95.4%), 1683 cm^{-1} (3.6%), and 1763 cm^{-1} (1.0%). This constitutes experimental evidence of the fact that organic bridges of U-1 were slightly less ordered than those of U-2.

Bands in the amide II region correspond to a mixed contribution of the N−H in-plane bending and C−N and C−C stretching vibrations.[32] This band was present at 1577 cm^{-1} in the urea-bridged silsesquioxanes bearing 9−12 methylene groups between both urea groups.[20] The strength of the H-bonds may be associated with the difference in the frequencies of maxima of amide I and amide II bands.[33−35] Small $\Delta\nu$ values (on the order of 40−60 cm^{-1}) are related to strong H-bonds, while $\Delta\nu$ values in the range 70−100 cm^{-1} are characteristic of less strong H-bonds.[18,20,21] Using the maximum of the fitted Lorentzian peaks, the resulting values for our samples are $\Delta\nu$(U-1) = 106 cm^{-1} and $\Delta\nu$(U-2) = 102 cm^{-1}. These values are located in the range where hydrogen bonds cannot be characterized as strong, with the more ordered sample (U-2) exhibiting a slightly higher value of the strength of these bonds.

Regarding the samples with urethane bridges, frequencies of maxima of the N−H stretching and the amide I bands are located in the region of H-bonded N−H and C═O groups.[26,36,37] A significant reduction in the intensity of the amide II band was observed for both Ut-1 and Ut-2 when compared to the urea-bridged silsesquioxanes (Figure 3). This can be assigned to a decrease in the hydrogen-bonding strength among urethane bridges when compared to urea bridges.[32] A spectral deconvolution of the C═O band was also performed in terms of the contribution of Lorentzian bands. The band of Ut-2 could be fitted with a single Lorentzian band peaking at 1705 cm^{-1}. The band of Ut-1 was composed of two Lorentzian bands at 1688 cm^{-1} (92.4%) and 1713 cm^{-1} (7.6%). This constitutes experimental evidence of the higher order present in the alignment of urethane bridges of Ut-2 when compared with those of Ut-1.

^{29}Si NMR Spectra. These spectra are useful to determine the fraction of Si atoms present in T_n groups (n = 0, 1, 2, or 3), where the subscript indicates the number of Si−O−Si bonds issuing from a particular Si atom. Figure 4 shows the ^{29}Si NMR spectra of U-2 and Ut-2 that were synthesized using a low formic acid concentration. Peaks at −49.0, −58.0, and −67.5 ppm in U-2 are respectively assigned to T_1, T_2, and T_3 structures.[11] Peaks at −58.1 and −66.4 ppm in Ut-2 are respectively assigned to T_2 and T_3 structures.

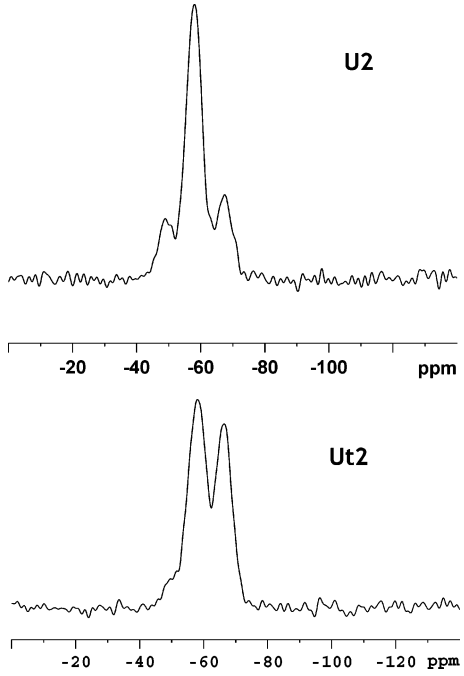

Figure 4. ^{29}Si NMR spectra of U-2 and Ut-2.

Table 3. Fraction of T_n Structures and Conversion in the Polycondensation Reaction of Urea- and Urethane-Bridged Silsesquioxanes

sample	T_1	T_2	T_3	conversion
U-1	0	0.510	0.490	0.830
U-2	0.124	0.696	0.180	0.685
Ut-1	0	0.440	0.560	0.853
Ut-2	0.057	0.518	0.425	0.789

Table 3 shows the fraction of T_n structures present in every one of the samples as well as the conversion in the polycondensation reaction defined as

$$x = \sum (n/3) T_n \qquad (1)$$

The urea-bridged silsesquioxanes exhibited a significant difference in the distribution of T_n structures. For U-2 the fraction of T_2 structures was significantly higher than those of T_1 and T_3 structures. This may be explained by the low rate of formation of Si−O−Si bonds compared to the rate of self-assembly of organic bridges. Once the organic bridges are self-assembled as in the scheme shown in Figure 2, it is possible to bond the Si atoms present at each side of the self-assembled structure through Si−O−Si bonds without affecting significantly the whole structure. This would convert the intermediate Si atoms into T_2 groups and the Si atoms present at the ends of the self-assembled structure into T_1 groups. Eventually, free SiOH groups of different assemblies may react among themselves leading to the observed small fraction of T_3 groups. A constant distance between organic bridges would be present in the different assemblies leading to the single band for the H-bonded C═O groups observed in the FTIR spectrum.

The situation is quite different for U-1 where the fast rate of polycondensation competes with the rate of self-assembly of organic bridges. The fast formation of Si−O−Si bonds restricts the attainment of a perfect arrangement of organic bridges leading to a distribution of distances among organic bridges pertaining to the same self-assembled structure. This in turn leads to an increase in the broadness of the band of the H-bonded C═O groups in the FTIR spectrum. A high fraction of both T_2 and T_3 structures is present in this sample with practically no residual T_1 groups.

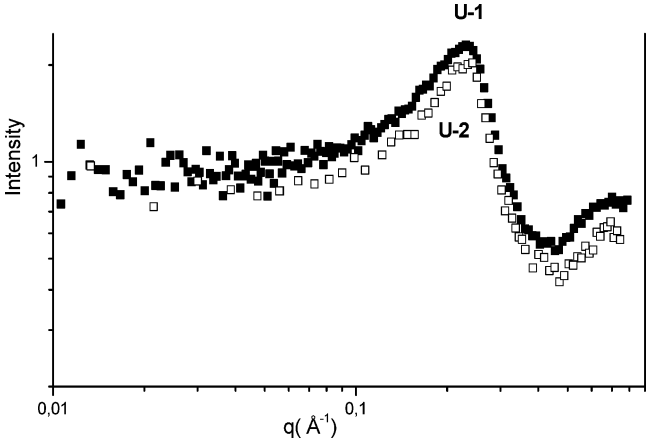

Figure 5. SAXS intensity curves for urea-bridged silsesquioxanes (U-1: filled squares; U-2: unfilled squares).

The trend for urethane-bridged silsesquioxanes is similar but much less marked. In this case the rate of self-assembly of organic domains is lower than in the case of urea-bridged silsesquioxanes due to the lower strength of the corresponding H-bonds. Therefore, even when using low formic acid concentrations (Ut-2), the rate of formation of Si−O−Si bonds is comparable to the rate of self-assembly of the organic bridges. This leads to a relative high fraction of T_3 groups present in Ut-2. For the formulation synthesized employing a high formic acid concentration (Ut-1), the polycondensation proceeds at a fast rate leading to a more disordered organic structure as reflected by the increase in the broadness of the band of H-bonded C═O groups in the FTIR spectrum.

The order attained in the self-assembly of organic bridges may be evaluated with SAXS spectra.

Small-Angle X-ray Scattering. SAXS is particularly adequate for studying the structure of bridged silsesquioxanes because of the contrast of electronic densities between the organic and inorganic phases. In the case of bridged silsesquioxanes exhibiting a self-assembly of the organic chains, an interference maximum in SAXS profiles appears with a characteristic distance equal to the length of the organic bridge.[22,38−41] An average size of the inorganic clusters can be estimated from the asymptotic behavior at low values of the scattering vector (q), and the presence of aggregates of primary inorganic particles in the inorganic clusters can also be analyzed.[42]

Figure 5 shows the SAXS spectra of the two urea-bridged silsesquioxanes. For both samples a peak corresponding to an interference maximum was observed at $q = 0.23$ Å^{-1}, determining a correlation distance of 27 Å between inorganic clusters. The distance between Si atoms located at both extremes of the organic bridge was estimated as follows. First, a cyclic structure composed of two parallel organic bridges joined at both ends by C−O−C bonds was built up, where the C atoms that replace the Si atoms at the end of each bridge are also bonded to two OH groups. This structure was optimized with the software ACD Labs/Chemsketch 3.5, which takes into account bond stretching, angle bending, internal rotation, and van der Waals nonbonded interactions but does not allow using Si atoms. Once the structure was optimized, terminal C atoms were again replaced by the corresponding Si atoms, and the distance between those located at the extremes of the organic bridge was calculated using the software ACD Labs/3D Viewer. The resulting value

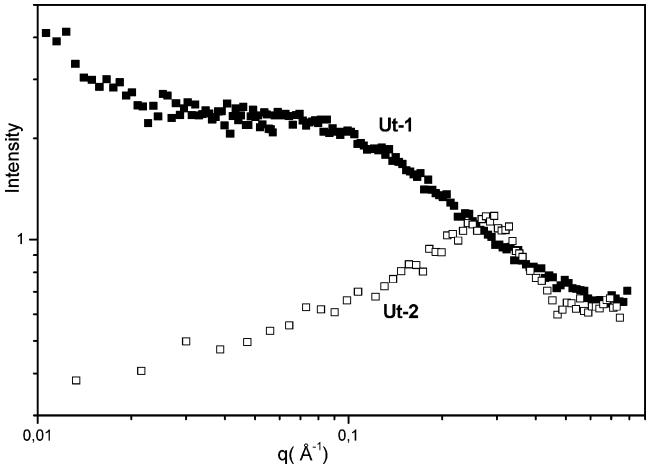

Figure 6. SAXS intensity curves for urethane-bridged silsesquioxanes (Ut-1: filled squares; Ut-2: unfilled squares).

was 25 Å, in good agreement with the experimental correlation distance of 27 Å.

Therefore, even in the case of carrying out a fast inorganic polycondensation (U-1), the rate of self-assembly of organic bridges is fast enough to produce ordering of the organic domains generating an interference maximum in the SAXS spectrum. The origin of such a rapid organization cannot be entirely ascribed to the formation of H-bonds because their strength was not very high as discussed when analyzing the FTIR spectra. A possible explanation of the fast structuring is via cooperative weak interactions between H-bonding of urea groups combined with the π-stacking of the three aromatic rings present in the structure of the bridge.[17,18,20]

For both U-1 and U-2 no harmonics were observed at higher values of q, indicating that both materials exhibit an amorphous character with a short-range ordered structure. The level of order, even if restricted to a short range, may be estimated from the width of the interference peak at half of its maximum, Δq, that determines a correlation length (ζ):[19]

$$\zeta = 2\pi/\Delta q$$

This distance corresponds to the periodicity in the stacking of lamella alternating inorganic and organic layers.[19] For urea-bridged silsesquioxanes exhibiting long-range structural ordering, experimental values of ζ were comprised in the range of 200−330 Å, whereas when the same precursors were not well-organized in alternating organic−inorganic lamella, values of ζ were in the range of 2−2.5 times the length of the organic spacer.[19] Values of the correlation length estimated from the SAXS spectra of Figure 5, were ζ(U-1) = 49 Å and ζ(U-2) = 54 Å, indicating the absence of a long-range structural ordering. The higher value of ζ for sample U-2 supports results from FTIR and ^{29}Si NMR spectra, indicating that presence of a more regularly organized structure in U-2 than in U-1.

Figure 6 shows the SAXS spectra of the urethane-bridged silsesquioxanes. In this case the driving force for the self-assembly of organic domains was not as intense as in the case of urea-bridged silsesquioxanes, possibly due to the lower strength of H-bonds and the fact that two instead of three aromatic rings are part of the bridge structure. The result was that the self-assembly of organic bridges could only be produced when employing a low rate of the inorganic polycondensation (Ut-2). A fast inorganic polycondensation led to the absence of an interference maximum in the SAXS spectrum (Ut-1).

For Ut-2 the interference peak at $q = 0.28$ Å^{-1} represents a characteristic length of 22.4 Å. The distance between Si atoms located at the extremes of the organic bridge was estimated employing a similar method than that used for the urea-bridged silsesquioxane, except that the optimization was based on three organic bridges joined at their ends by C−O−C−O−C bonds. (C atoms replaced Si atoms in the optimization process and are also bonded to OH groups to complete the chemical structure.) After optimization of the chemical structure terminal C atoms were replaced by Si atoms, and the distance between them was calculated. This led to a value of 21.5 Å, in very good agreement with the experimental characteristic length.

The SAXS intensity curve of Ut-1 shows an intensity plateau and the growth of intensity at low angles. Such a type of intensity profile could be interpreted by an association of small inorganic clusters into large aggregates. The radius of the small clusters was estimated as a value close to 10 Å using the Guinier analysis of the desmeared data in the q range of 0.03−0.2 Å^{-1}. This value could be slightly underestimated due to the finite silsesquioxane concentration. The increase of intensity at low q values (<0.03 Å^{-1}) over the plateau intensity originated by the small clusters can be assigned to a Porod's law contribution of the scattering of large aggregates of radius higher than 400 Å. Therefore, the fast inorganic polycondensation in sample Ut-1 led to the generation of small inorganic clusters that were further aggregated into large clusters. However, no spatial correlation was found, implying that the aggregation occurs at random and is not organized by the presence of the organic bridges.

We can now analyze how these different nanostructures affect the photoluminescence spectra of the bridged silsesquioxanes.

Photoluminescence Spectra. The photoluminescence spectra of the aromatic precursors were first analyzed. The urea precursor exhibited emission bands at 306 and 321 nm when excited at wavelengths comprised in the range 250−290 nm. The urethane precursor showed emission bands at 306 and 342 nm in the same range of excitation wavelengths. To avoid the photoluminescence of the aromatic rings, excitation wavelengths used to analyze the emission spectra were always equal to or higher than 330 nm.

We will start the analysis with sample U-2, which according to FTIR, ^{29}Si NMR, and SAXS spectra exhibits self-assembled structures with a regular order between the organic bridges. Photoluminescence spectra (Figure 7) showed the presence of two main contributions: a band at about 445 nm that appeared when the excitation wavelength was comprised between 330 and 350 nm and a second band with a maximum shifting from about 475 to 495 nm when varying the excitation wavelength in the range 330−400 nm. Increasing λ_{exc} up to 400 nm produced a decrease of the intensity of the band at 445 nm and an increase in the intensity of the second band. The maximum intensity was observed for λ_{exc} in the range 385−400 nm, with emission bands peaking at about 485−495 nm. On the basis of the analysis of Carlos et al.,[25] the purplish-blue band at 445 nm might be assigned to radiative recombinations that occur within the nanometer-sized inorganic clusters, and the blue band at 475−495 nm might be assigned to a photoinduced proton transfer generating NH_2^+ and N^- defects and their subsequent radiative recombination.

Figure 8 shows excitation spectra of U-2 for emission wavelengths comprised between 445 and 490 nm. Broad bands are observed with maxima shifting to the red when increasing the emission wavelength. Spectra deconvolution revealed the presence of two main bands. The first one is centered at 370 nm and corresponds to purplish-blue emission from the inorganic

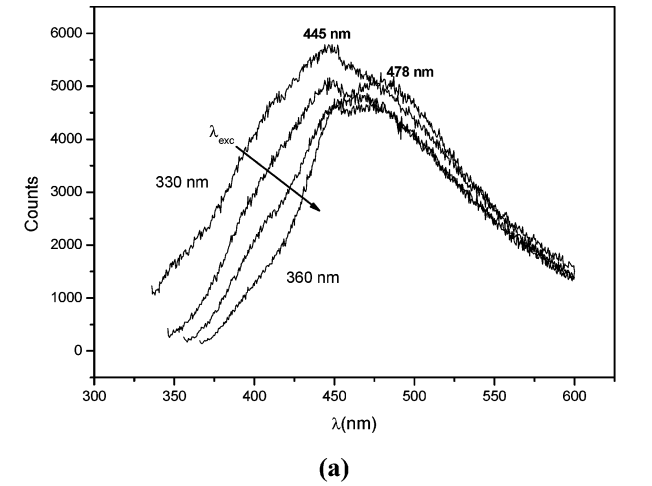

(a)

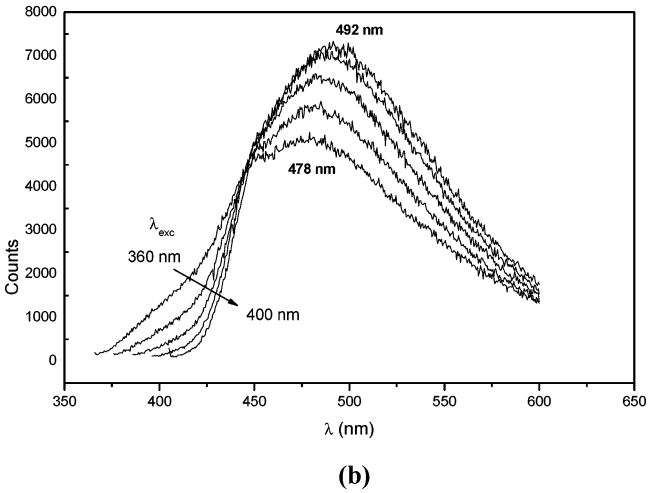

(b)

Figure 7. Photoluminescence spectra of U-2: (a) excitation wavelengths between 330 and 360 nm; (b) excitation wavelengths between 360 and 400 nm.

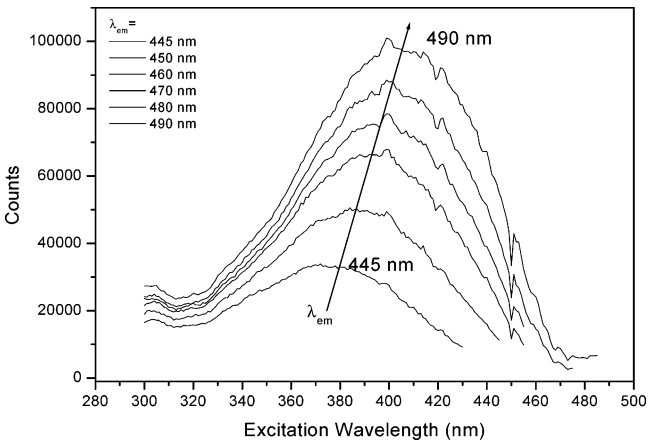

Figure 8. Excitation spectra of U-2 for emission wavelengths comprised in the 445−490 nm range.

clusters. The second one shifts from 395 to 415 nm and corresponds to the blue photoluminescence band assigned to the photoinduced proton transfer generating NH_2^+ and N^- defects and their subsequent radiative recombination. The second band is the most important one for emission wavelengths higher than 460 nm. Therefore, the excitation spectra support the presence of two main components in the photoluminescence spectra. However, these results should be confirmed by time-resolved spectroscopy to unequivocally conclude about the number of distinct emission centers.

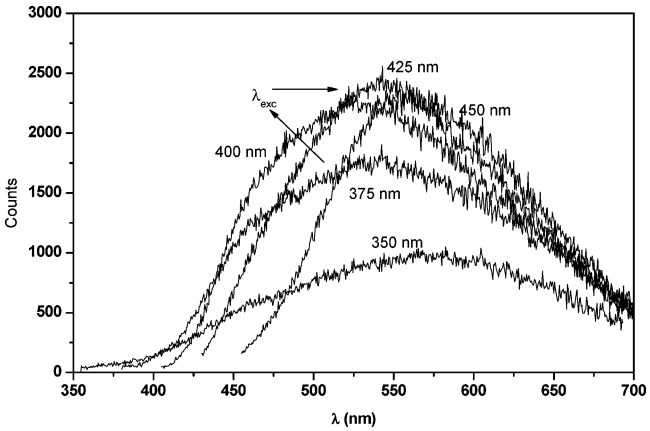

Figure 9. Photoluminescence spectra of U-1 for excitation wavelengths comprised in the 350−450 nm range.

Photoluminescence spectra of the urea-bridged silsesquioxane with less-ordered self-assembled structures (U-1) are shown in Figure 9. The maximum intensity was obtained for an excitation wavelength in the visible region (420 nm), giving a broad emission band covering practically the whole visible spectrum (maximum at 535 nm, in the green region). Therefore, U-1 converts blue light into white light, a fact that has potential technological applications.

The spectra exhibit different features than those of sample U-2, indicating their sensitivity to the level of ordering of the organic bridges. A Gaussian deconvolution of these spectra showed the presence of three different bands: one peaking at about 440 nm that appears when λ_{exc} is less than 380 nm and represents less than 5% of the total area, a second one at about 490 nm exhibiting a small red shift when increasing λ_{exc}, and a third one at about 590 nm exhibiting a higher red shift with the increase in λ_{exc}.

A distinctive characteristic of these spectra is the blue shift of the maximum observed when increasing the excitation wavelength from 350 to 400 nm, followed by a pronounced red shift when increasing further the excitation wavelength. This indicates the existence of at least two different types of emission centers in this range of wavelengths. Those giving a maximum at about 490 nm in the emission spectra are assigned to the radiative recombination of NH_2^+ and N^- defects present in ordered organic domains of the same type as those present in U-2. This is confirmed by the fact that the maximum in the excitation spectra of these centers was observed for excitation wavelengths close to 400 nm (as for U-2). The intensity of the corresponding excitation band decays sharply either increasing or decreasing the excitation wavelength by 50 nm (Figure 8). This is expected for a localized process taking place in the regularly ordered organic bridges. Overlapped with this localized emission process there is another photoluminescence band corresponding to emission centers exhibiting a broad excitation band. A possible origin of this band is the photoinduced proton transfer involving H-bonds exhibiting a broad energy distribution present in less-ordered self-assemblies of organic bridges. Except in the range of excitation wavelengths close to 400 nm where the emission from ordered organic domains is predominant, the less-ordered domains are responsible for the largest contribution to the photoluminescence spectra. This explains why there is an initial blue shift of the maximum followed by a red shift. Therefore, ordered and less-ordered self-assembled structures should coexist in sample U-2. The fraction of ordered domains was probably generated at low conversions when the fraction of T_3 structures was not yet important.

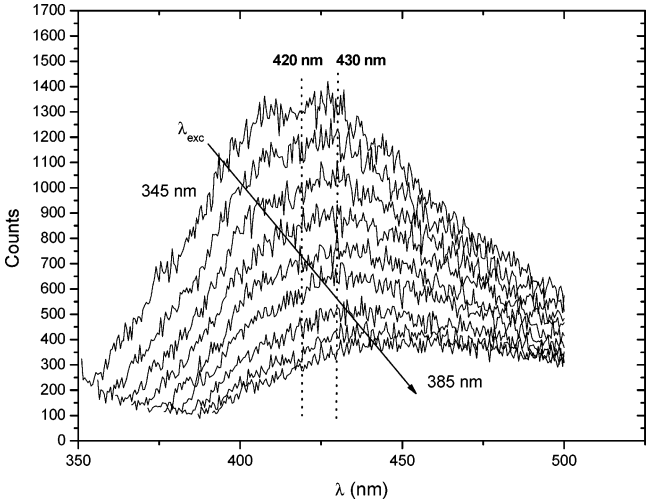

Figure 10. Photoluminescence spectra of Ut-2 for excitation wavelengths comprised in the 345−385 nm range.

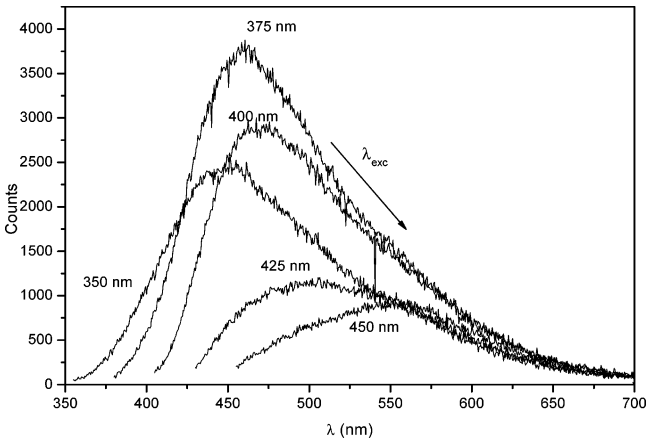

Figure 11. Photoluminescence spectra of Ut-1 for excitation wavelengths comprised in the 350−450 nm range.

Figure 10 shows the photoluminescence spectra of Ut-2 exhibiting self-assembled organic bridges. Now, only the band at 420−430 nm is important, decreasing rapidly in intensity when increasing λ_{exc}. The excitation spectra obtained at constant emission wavelengths in the range 420−460 nm showed two main contributions at 330 and 370 nm, in the region of radiative recombinations that occur within inorganic clusters. No significant photoluminescence seems to be originated by the generation of charged groups in H-bonds as in the urea-bridged silsesquioxanes. This led to a weak intensity of the photoluminescence spectra.

Photoluminescence spectra of Ut-1 exhibiting no order in the self-assembly of organic bridges were significantly different than those of sample Ut-2 (Figure 11). A band with a broad energy distribution appeared in the spectra, with a pronounced red shift when increasing λ_{exc}. The excitation spectra showed a maximum at 380 nm with a slight red shift when increasing the emission wavelength. The higher intensity and broader energy distribution of the emission spectra of Ut-2 when compared to Ut-1 could be the result of the presence of large inorganic domains generated by aggregates of small inorganic clusters. According to Brankova et al.,[24] smaller inorganic clusters tend to absorb and emit at shorter wavelengths than large inorganic clusters due to size effects. An increase in the size of inorganic clusters produced by maturing a gel based on (aminopropyl)triethoxysilane led to a red shift in the emission spectra when the excitation was performed at longer wavelengths.[24] This is consistent with the changes observed in the structures and photoluminescence spectra of samples Ut-1 and Ut-2.

Conclusions

The nanostructure generated during the synthesis of aromatic urea- and urethane-bridged silsesquioxanes is determined by the competition between the order produced by the self-assembly of organic domains and the disorder introduced by the inorganic polycondensation. In the case of urea-bridged silsesquioxanes the driving force for the organization of organic groups was high enough to generate a distribution of self-assembled structures even with a competition of a fast inorganic polycondensation. However, the arrangement was more regular and the short-range order higher when the rate of inorganic polycondensation was lower. This was proved by deconvolution of the C═O band in FTIR spectra, by the relative amounts of T_1, T_2, and T_3 structures present in ^{29}Si NMR spectra and by the broadness of interference peaks in SAXS spectra. The photoluminescence spectra of the most ordered structures revealed the presence of two main processes: radiative recombinations within inorganic clusters (maximum at an excitation wavelength close to 370 nm) and photoinduced proton transfer generating NH_2^+ and N^- defects and their subsequent radiative recombination (maximum at an excitation wavelength close to 400 nm). In the less-ordered urea-bridged silsesquioxanes a third process characterized by broad emission and excitation bands was present. It was assigned to a photoinduced proton transfer in H-bonds exhibiting a broad range of strengths. This implies that both well-organized and less-regular self-assembled structures are present in the final material, the former being presumably formed in the initial stages of the polycondensation reaction.

For urethane-bridged silsesquioxanes the driving force for the self-assembly of organic bridges was not as high as in the case of urea-bridged silsesquioxanes. When the synthesis was performed with a high rate of the inorganic polycondensation, self-assembled structures were not produced. Instead, large inorganic domains composed of small inorganic clusters were generated. Self-assembly of organic domains took only place when employing low polycondensation rates. For both materials the photoluminescence was mainly due to radiative processes within inorganic clusters. The sample where the self-assembly of organic domains generated small inorganic clusters exhibited a weak photoluminescence intensity whereas a higher intensity and a red shift of the spectra were observed for the material exhibiting large aggregates of inorganic clusters.

In conclusion, the nanostructuration produced in urea- and urethane-bridged silsesquioxanes could be controlled by varying the rate of the inorganic polycondensation. Changes in nanostructuration produce a significant effect on photoluminescence spectra, a fact that may be used either to generate desired emission spectra or, conversely, to monitor the order within the self-assembled structures.

Acknowledgment. The financial support of the National Research Council (CONICET, Argentina), the National Agency for the Promotion of Science and Technology (ANPCyT, Argentina, PICT 14738-03), the University of Mar del Plata, the Grant Agency of the Czech Republic (Project 203/05/2252), and Project Nanoter (Project MAT2004/01347, MEC-DGI, Spain) is gratefully acknowledged. INTEMA and the Institute of Macromolecular Chemistry acknowledge the support of the European Network of Excellence Nanofun-Poly for the diffusion of their research results.

References and Notes

(1) Shea, K. J.; Loy, D. A.; Webster, O. W. *J. Am. Chem. Soc.* **1992**, *114*, 6700.
(2) Loy, D. A.; Shea, K. J. *Chem. Rev.* **1995**, *95*, 1431.
(3) Judeinstein, P.; Sanchez, C. *J. Mater. Chem.* **1996**, *6*, 511.
(4) Cerveau, G.; Corriu, R. J. P. *Coord. Chem. Rev.* **1998**, *178*−*180*, 1051.
(5) Corriu, R. J. P. *Polyhedron* **1998**, *17*, 925.
(6) Barton, T. J.; Bull, L. M.; Klemperer, W. G.; Loy, D. A.; McEnaney, B.; Misono, M.; Monson, P. A.; Pez, G.; Scherer, G. W.; Vartuli, J. C.; Yaghi, O. M. *Chem. Mater.* **1999**, *11*, 2633.
(7) Cerveau, G.; Corriu, R. J. P.; Framery, E. *J. Mater. Chem.* **2000**, *10*, 1617.
(8) Cerveau, G.; Corriu, R. J. P.; Framery, E. *Polyhedron* **2000**, *19*, 307.
(9) Shea, K. J.; Loy, D. A. *Acc. Chem. Res.* **2001**, *34*, 707.
(10) Shea, K. J.; Loy, D. A. *MRS Bull.* **2001**, *26*, 368.
(11) Shea, K. J.; Loy, D. A. *Chem. Mater.* **2001**, *13*, 3306.
(12) Moreau, J. J. E.; Vellutini, L.; Wong Chi Man, M.; Bied, C. *J. Am. Chem. Soc.* **2001**, *123*, 1509.
(13) Moreau, J. J. E.; Vellutini, L.; Wong Chi Man, M.; Bied, C.; Bantignies, J. L.; Dieudonné, P.; Sauvajol, J. L. *J. Am. Chem. Soc.* **2001**, *123*, 7957.
(14) Dautel, O. J.; Lère-Porte, J. P.; Moreau, J. J. E.; Wong Chi Man, M. *Chem. Commun.* **2003**, 2662.
(15) Moreau, J. J. E.; Vellutini, L.; Wong Chi Man, M.; Bied, C. *Chem. Eur. J.* **2003**, *9*, 1594.
(16) Bied, C.; Moreau, J. J. E.; Vellutini, L.; Wong Chi Man, M. *J. Sol-Gel Sci. Technol.* **2003**, *26*, 583.
(17) Moreau, J. J. E.; Pichon, B. P.; Wong Chi Man, M.; Bied, C.; Pritzkow, H.; Bantignies, J. L.; Diedonné, P.; Sauvajol, J. L. *Angew. Chem., Int. Ed.* **2004**, *43*, 203.
(18) Moreau, J. J. E.; Pichon, B. P.; Bied, C.; Wong Chi Man, M. *J. Mater. Chem.* **2005**, *15*, 3929.
(19) Moreau, J. J. E.; Vellutini, L.; Dieudonné, P.; Wong Chi Man, M.; Bantignies, J. L.; Sauvajol, J. L.; Bied, C. *J. Mater. Chem.* **2005**, *15*, 4943.
(20) Moreau, J. J. E.; Vellutini, L.; Wong Chi Man, M.; Bied, C.; Dieudonné, P.; Bantignies, J. L.; Sauvajol, J. L. *Chem. Eur. J.* **2005**, *11*, 1527.
(21) Moreau, J. J. E.; Pichon, B. P.; Arrachart, G.; Wong Chi Man, M.; Bied, C. *New J. Chem.* **2005**, *29*, 653.
(22) Carlos, L. D.; de Zea Bermudez, V.; Sá Ferreira, R. A.; Marques, L.; Assunção, M. *Chem. Mater.* **1999**, *11*, 581.
(23) Carlos, L. D.; Sá Ferreira, R. A.; Orion, I.; de Zea Bermudez, V.; Rocha, J. *J. Lumin.* **2000**, *87*−*89*, 702.
(24) Brankova, T.; Bekiari, V.; Llanos, P. *Chem. Mater.* **2003**, *15*, 1855.
(25) Carlos, L. D.; Sá Ferreira, R. A.; Pereira, R. N.; Assunção, M.; de Zea Bermudez, V. *J. Phys. Chem. B* **2004**, *108*, 14924.
(26) Fu, L.; Sá Ferreira, R. A.; Silva, N. J. O.; Carlos, L. D.; de Zea Bermudez, V.; Rocha, J. *Chem. Mater.* **2004**, *16*, 1507.
(27) Eisenberg, P.; Erra-Balsells, R.; Ishikawa, Y.; Lucas, J. C.; Nonami, H.; Williams, R. J. J. *Macromolecules* **2002**, *35*, 1160.
(28) Sharp, K. *J. Sol-Gel Sci. Technol.* **1994**, *2*, 35.
(29) Stewart, J. E. *J. Chem. Phys.* **1959**, *30*, 1259.
(30) Smith, A. L. *Spectrochim. Acta* **1960**, *16*, 87.
(31) Chiang, C. H.; Ishida, H.; Koenig, J. L. *J. Colloid Interface Sci.* **1980**, *74*, 396.
(32) de Zea Bermudez, V.; Carlos, L. D.; Alcácer, L. *Chem. Mater.* **1999**, *11*, 569.
(33) Jadzyn, J.; Stockhauser, M.; Zywucki, B. *J. Phys. Chem.* **1987**, *91*, 754.
(34) de Loos, M.; van Esch, J.; Stokroos, I.; Kellogg, R. M.; Feringa, B. L. *J. Am. Chem. Soc.* **1997**, *119*, 12675.
(35) van Esch, J.; Schoonbeck, F.; de Loos, M.; Kooijman, H.; Spek, A. L.; Kellogg, R. M.; Feringa, B. L. *Chem. Eur. J.* **1999**, *5*, 937.
(36) Coleman, M. M.; Skrovanek, D. J.; Hu, J.; Painter, P. C. *Macromolecules* **1988**, *21*, 59.
(37) Coleman, M. M.; Lee, K. H.; Skrovanek, D. J.; Painter, P. C. *Macromolecules* **1986**, *19*, 2149.
(38) Rodrigues, D. E.; Brennan, A. B.; Betrabet, C.; Wang, B.; Wilkes, G. L. *Chem. Mater.* **1992**, *4*, 1437.
(39) Dahmouche, K.; Santilli, C. V.; Pulcinelli, S. H.; Craievich, A. F. *J. Phys. Chem. B* **1999**, *103*, 4937.
(40) Molina, C.; Ribeiro, S. J. L.; Dahmouche, K.; Santilli, C. V.; Craievich, A. F. *J. Sol-Gel Sci. Technol.* **2000**, *19*, 615.
(41) Dahmouche, K.; Carlos, L. D.; de Zea Bermudez, V.; Sá Ferreira, R. A.; Santilli, C. V.; Craievich, A. F. *J. Mater. Chem.* **2001**, *11*, 3249.
(42) Krakovsky, I.; Urakawa, H.; Kajiwara, K.; Kohjiya, S. *J. Non-Cryst. Solids* **1998**, *231*, 31.

MA052105Y